

Nonlinear Optical Properties and Luminescence of Solid Solutions of $\text{Li}_{1-x}(\text{Nb,Ta})_{1-x}\text{W}_x\text{O}_3$

M. Wiegel,* M. H. J. Emond, T. H. M. de Bruin, and G. Blasse

Debye Institute, Utrecht University, Department of Condensed Matter, POB 80.000,
3508 TA Utrecht, The Netherlands

Received February 11, 1994. Revised Manuscript Received April 28, 1994*

The nonlinear optical response of $\text{Li}_{1-x}(\text{Nb,Ta})_{1-x}\text{W}_x\text{O}_3$ increases strongly with x . This is explained in terms of changing bond polarizabilities: W-O bonds are more polarizable than Nb-O/Ta-O bonds. A W-O bond polarizability β^{\parallel} of $(570 \pm 130) 10^{-40} \text{ m}^4/\text{V}$ is derived, neglecting β^{\perp} . The luminescence properties depend also on x , and new emission and excitation bands are found.

Introduction

Laser-diode second harmonic generation (SHG) devices or blue laser sources are expected to be of large importance in future optoelectronic applications. Some of the best inorganic frequency-doubling materials can be found among compounds with the LiNbO_3 structure. Doping of LiNbO_3 and LiTaO_3 has been studied in relation with optical damage (photorefractive effect).^{1,2} However, doping may influence also the nonlinear optical (NLO) response of a material.³⁻⁵

According to a relatively simple model derived by Bergman and Crane in 1975,⁶ the NLO response depends largely on microscopic NLO bond polarizabilities and geometrical factors. If substitution does not significantly alter the structure of a material, the SHG response will approximately be a function of the NLO bond polarizabilities only.

From the literature⁷⁻⁹ it is known that LiTaO_3 and LiNbO_3 form a solid solution series with WO_3 from 0 to 30 and 50 mol %, respectively. There also exists a solid solution series with MoO_3 , but it extends only to about 10 and 20 mol % for LiTaO_3 and LiNbO_3 , respectively.⁷

Since the difference in electronegativity between W/Mo and O is smaller than that between Nb/Ta and O, the W-O/Mo-O bonds are expected to be more covalent and to have a higher NLO bond polarizability than the Nb-O/Ta-O bonds. In this work the NLO properties of LiNbO_3 and LiTaO_3 are studied as a function of the WO_3 content.

To monitor the defect chemistry of the $\text{Li}_{1-x}(\text{Nb,Ta})_{1-x}\text{W}_x\text{O}_3$ solid solutions the luminescence is also studied as a function of x , as the luminescence properties of undoped LiNbO_3 and LiTaO_3 depend strongly on the

stoichiometry of the samples. Stoichiometric LiTaO_3 , for instance, shows an emission band with a maximum at 340 nm ($\lambda_{\text{exc}} = 235$ nm), whereas Li-deficient samples emit at ~ 500 nm ($\lambda_{\text{exc}} = 260$ nm).¹⁰ LiNbO_3 shows a similar behavior. The intrinsic niobate emission lies at 440 nm ($\lambda_{\text{exc}} = 260$ nm), whereas the extrinsic emission has its maximum at ~ 520 nm ($\lambda_{\text{exc}} = 305$ nm).^{2,11,12}

The results of the SHG and luminescence measurements of the solid solution series with MoO_3 will not be discussed here, since they are comparable to those of the tungstate series, and the solubility of MoO_3 is low.

Experimental Section

Preparation. Solid solutions of $\text{Li}_{1-x}\text{Nb}_{1-x}\text{W}_x\text{O}_3$ were prepared by firing intimate mixtures of Li_2CO_3 (Merck, suprapur), Nb_2O_5 (Starck, ultrapure), and WO_3 (Merck, p.a.) in the stoichiometric ratio with a 5 mol % excess of Li_2CO_3 at 750 °C for 8 h in air. The products were milled again and fired for 8 h at 800 °C. A platinum-rhodium crucible was used. If $x > 0.50$, a trirutile phase is obtained.^{7,8}

The preparation of the solid solution series $\text{Li}_{1-x}\text{Ta}_{1-x}\text{W}_x\text{O}_3$ is very similar, but the firing temperatures are lower: 650 and 700 °C, respectively. In contrast to earlier reports in the literature,⁹ for $x > 0.25$ evidence of the formation of a trirutile second phase is found in the X-ray diffraction patterns.

All powdered samples were checked by X-ray powder diffraction and were found to be single phase.

Differential Thermal Analysis (DTA) Measurements. On some of the $\text{Li}_{1-x}\text{Nb}_{1-x}\text{W}_x\text{O}_3$ samples DTA measurements (heating rate 10 °C/min) were performed. $\text{Li}_{0.5}\text{Nb}_{0.5}\text{W}_{0.5}\text{O}_3$ shows three endothermic peaks, at 680, 700, and 890 °C. The latter is due to the decomposition into NbW_2O_6 and Li_2WO_4 .⁸ For samples with $x \leq 0.25$ no decomposition is observed below 1200 °C.

Instrumentation. All optical measurements were performed as described before,¹³ using a Spex fluorolog spectrofluorometer with an Oxford liquid helium flow cryostat. Diffuse reflection spectra of the powdered samples were measured on a double-beam Perkin-Elmer Lambda 7 UV-vis spectrophotometer at room temperature.

Effective nonlinear optical tensor coefficients (d_{eff}) were measured with a second harmonic analyzer (Philips), which is equipped with a pulsed Nd^{3+} glass laser ($\lambda = 1064$ nm) and suitable for measuring crystalline powdered samples.¹⁴

* Abstract published in *Advance ACS Abstracts*, June 1, 1994.
(1) Schirmer, O. F.; Thiemann, O.; Wöhlecke, M. *J. Phys. Chem. Solids* 1991, 52, 185.
(2) Fischer, C.; Wöhlecke, M.; Volk, T.; Rubina, N. *Phys. Status Solidi A* 1993, 137, 247.
(3) McCarron III, E. M.; Calabrese, J. C.; Gier, T. E.; Cheng, L. K.; Foris, C. M.; Bierlein, J. D. *J. Solid State Chem.* 1993, 102, 354.
(4) Thomas, P. A.; Watts, B. E. *Solid State Commun.* 1990, 73, 97.
(5) Phillips, M. L. F.; Harrison, W. T. A.; Stucky, G. D.; McCarron III, E. M.; Calabrese, J. C.; Gier, T. E. *Chem. Mater.* 1992, 4, 222.
(6) Bergman, J. G.; Crane, C. R. *J. Solid State Chem.* 1975, 12, 172.
(7) Blasse, G.; de Pauw, A. D. M. *J. Inorg. Nucl. Chem.* 1970, 32, 3960.
(8) Fourquet, J. L.; Le Bail, A.; Gillet, P. A. *Mater. Res. Bul.* 1988, 23, 1163.
(9) Kawakami, S.; Tsuzuki, A.; Sekiya, T.; Ishikuro, I.; Masuda, M.; Torii, Y. *Mater. Res. Bul.* 1985, 20, 1435.

(10) Krol, D. M.; Blasse, G.; Powell, R. C. *J. Chem. Phys.* 1980, 73, 163.

(11) Emond, M. H. J.; Wiegel, M.; Blasse, G.; Feigelson, R. *Mater. Res. Bul.* 1993, 28, 1025.

(12) Wiegel, M.; Emond, M. H. J.; Stobbe, E. R.; Blasse, G. *J. Phys. Chem. Solids*, submitted.

(13) Wiegel, M.; Blasse, G. *J. Solid State Chem.* 1992, 99, 388.

(14) Dougherty, J. P.; Kurtz, S. K. *J. Appl. Crystallogr.* 1976, 9, 145.

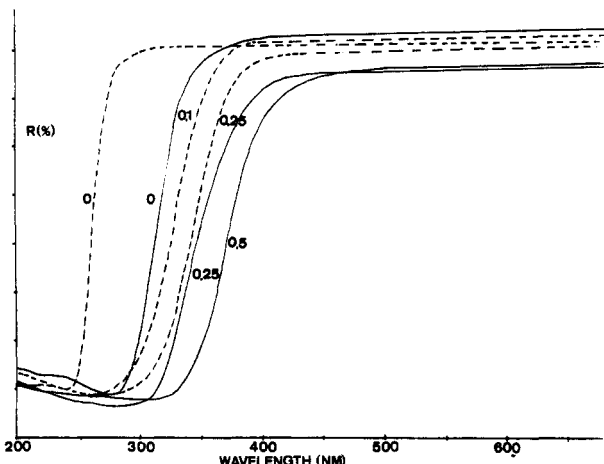


Figure 1. Diffuse reflection spectra of $\text{Li}_{1-x}(\text{Nb,Ta})_{1-x}\text{W}_x\text{O}_3$ at room temperature. The solid curves represent the spectra of $\text{Li}_{1-x}\text{Nb}_{1-x}\text{W}_x\text{O}_3$, whereas the broken curves are the spectra of $\text{Li}_{1-x}\text{Ta}_{1-x}\text{W}_x\text{O}_3$.

The SHG efficiency of powders depends strongly on the particle size,¹⁴ so it was made sure that the frequency-doubled light was collected from samples of a comparable, uniform particle size between 3 and 5 μm , which had been carefully checked with a microscope.

To minimize the scattering, the sample powders were mixed with index-matching fluids (Cargill, Inc.) of a comparable refractive index. If the refractive index of an index-matching fluid does not match that of the sample, the measured SHG response will be too low.¹⁴ However, changes in the refractive indices of the samples, due to a different WO_3 content, were not important here: varying the refractive index of the index-matching fluids from 1.7 to 2.0 did not result in a higher or a lower SHG response.

The SHG intensity was measured relative to stoichiometric LiNbO_3 and LiTaO_3 powder standards.

Results

Luminescence. Figure 1 shows some of the diffuse reflection spectra of $\text{Li}_{1-x}\text{Nb}_{1-x}\text{W}_x\text{O}_3$ ($0 \leq x \leq 0.5$) at room temperature (RT). The optical absorption edge, which can be obtained by extrapolating the slope of the absorption curve, depends on the value of x : it shifts from 280 nm ($x = 0$) to 350 nm ($x = 0.5$). For the solid solutions $\text{Li}_{1-x}\text{Ta}_{1-x}\text{W}_x\text{O}_3$ with $0 \leq x \leq 0.25$ a similar dependence is found (see also Figure 1).

Compositions $\text{Li}_{1-x}\text{Nb}_{1-x}\text{W}_x\text{O}_3$ ($0 \leq x \leq 0.5$) show strong luminescence at 4.2 K. As a representative example, some of the excitation and emission spectra of the luminescence of $\text{Li}_{1-x}\text{Nb}_{1-x}\text{W}_x\text{O}_3$ at 4.2 K are given in Figure 2.

The excitation and emission spectra are complicated: there are several broad bands present. For $x = 0.50$ the excitation spectrum shows two bands with maxima at 275 and 310 nm. Short-wavelength excitation ($\lambda_{\text{exc}} = 275$ nm) gives an emission with a maximum at 520 nm. Long-wavelength excitation ($\lambda_{\text{exc}} = 310$ nm) gives an emission with a maximum at 570 nm. The $T_{1/2}$ value (the temperature at which the luminescence intensity has dropped to 50% of its intensity at 4.2 K) of the "520 nm" emission band is 55 K, whereas that of the "570-nm" emission band is 30 K.

The luminescence properties of the $\text{Li}_{1-x}\text{Nb}_{1-x}\text{W}_x\text{O}_3$ solid solutions depend strongly on x . Samples with low x show an additional emission band with a maximum at 440 nm ($\lambda_{\text{exc}} = 260$ nm; see also Figure 2). The $T_{1/2}$ value is ~ 200

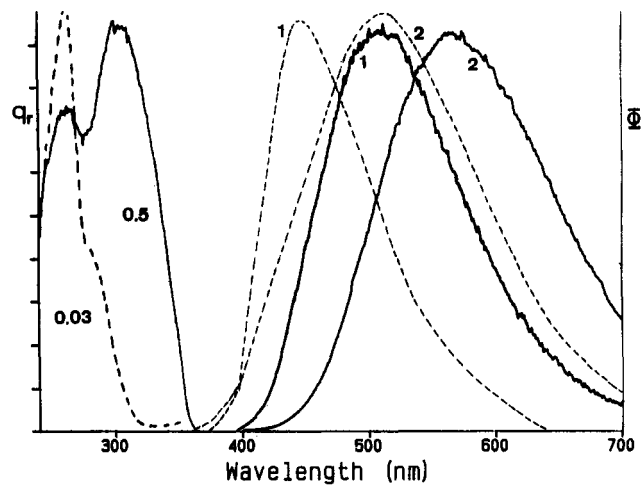


Figure 2. Some excitation and emission spectra of the luminescence of $\text{Li}_{1-x}\text{Nb}_{1-x}\text{W}_x\text{O}_3$ at 4.2 K. Φ denotes the spectral radiant power per constant wavelength interval, and q_r gives the relative quantum output. The broken curves are the spectra for $x = 0.03$, whereas the solid curves represent the spectra for $x = 0.50$. Excitation is into the shorter wavelength excitation band (curves 1) or in the longer wavelength excitation band (curves 2). The excitation spectra are monitored for the emission wavelength 440 nm ($x = 0.03$) and 540 nm ($x = 0.50$).

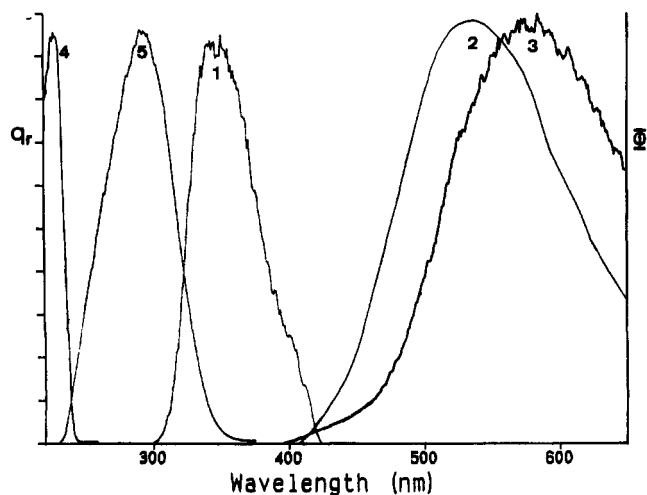


Figure 3. Excitation and emission spectra of the luminescence of $\text{Li}_{0.9}\text{Ta}_{0.9}\text{W}_{0.1}\text{O}_3$ at 4.2 K. The excitation wavelengths are 235 nm (curve 1), 290 nm (curve 2), and 320 nm (curve 3). The emission wavelengths are 340 nm (curve 4) and 580 nm (curve 5).

K. This emission is similar to what has been observed for stoichiometric (undoped) LiNbO_3 samples^{2,11} and is, therefore, ascribed to intrinsic niobate groups. If x increases, the intrinsic niobate emission disappears. The maxima of the other emission bands shift to longer wavelengths for increasing x .

The luminescence properties of $\text{Li}_{1-x}\text{Ta}_{1-x}\text{W}_x\text{O}_3$ ($0 \leq x \leq 0.25$) show some remarkable similarities to those of $\text{Li}_{1-x}\text{Nb}_{1-x}\text{W}_x\text{O}_3$ ($0 \leq x \leq 0.5$). For instance, if x is low, intrinsic tantalate emission with a maximum at 340 nm ($\lambda_{\text{exc}} = 235$ nm) and a $T_{1/2}$ value of ~ 100 K is observed.¹² At higher x values this emission becomes weaker.

In Figure 3 the excitation and emission spectra of $\text{Li}_{0.9}\text{Ta}_{0.9}\text{W}_{0.1}\text{O}_3$ at 4.2 K are shown. There are two excitation bands with maxima at 235 and ~ 290 nm, respectively. Excitation at ~ 290 nm gives an emission band with a maximum at 540 nm. The $T_{1/2}$ value of this emission is 55 K. Longer wavelength excitation ($\lambda_{\text{exc}} = 320$ nm) gives

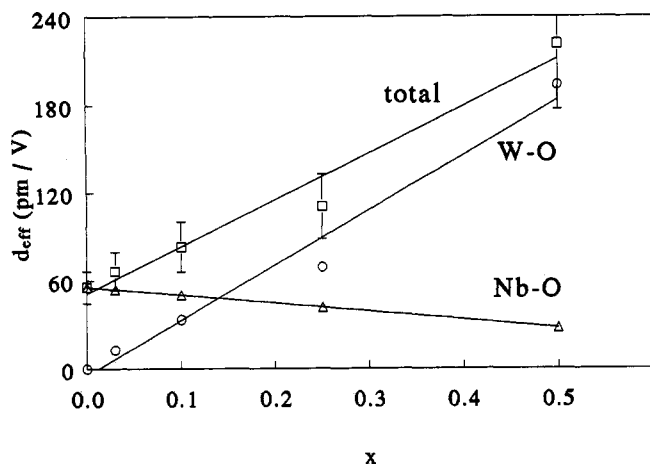


Figure 4. Absolute NLO response of $\text{Li}_{1-x}\text{Nb}_{1-x}\text{W}_x\text{O}_3$ as a function of x . The curve "total" gives the total NLO response. The curves "Nb-O" and "W-O" represent the NLO response due to the Nb-O and W-O bonds, respectively.

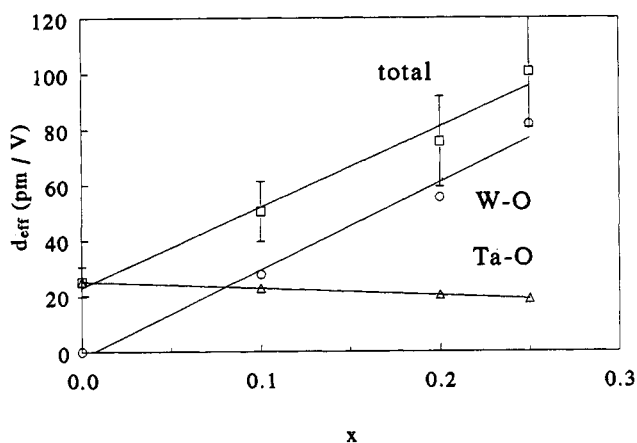


Figure 5. Absolute NLO response of $\text{Li}_{1-x}\text{Ta}_{1-x}\text{W}_x\text{O}_3$ as a function of x . The curve "total" gives the total NLO response, whereas the curves "Ta-O" and "W-O" give the NLO response due to the Ta-O and W-O bonds, respectively.

an emission band with a maximum at 580 nm (see also Figure 3).

Nonlinear Optical Properties. The phase matchable tensor coefficient d_{33} of stoichiometric LiNbO_3 was calculated on the basis of data on d_{33} of congruently grown Li-deficient crystals¹⁵ (with $d_{33}(\text{KH}_2\text{PO}_4) = 0.63 \text{ pm/V}$)¹⁶ using the bond parameter model of Bergman and Crane.⁶ It amounts to -55.4 pm/V . Congruently grown LiTaO_3 crystals tend to be Li-poor also.¹² However, the d_{33} of stoichiometric LiTaO_3 could not be calculated, since crystallographic data about stoichiometric LiTaO_3 is lacking in the literature. Therefore, the literature value of -25.2 pm/V was used.¹⁷ These d_{33} values are used to estimate the NLO response of the $\text{Li}_{1-x}(\text{Ta,Nb})_{1-x}\text{W}_x\text{O}_3$ samples.

The results of the powder SHG measurements on $\text{Li}_{1-x}\text{Nb}_{1-x}\text{W}_x\text{O}_3$ and $\text{Li}_{1-x}\text{Ta}_{1-x}\text{W}_x\text{O}_3$ are presented in Figures 4 and 5. The NLO response increases linearly with x .

Discussion

Luminescence. Introduction of WO_3 in $\text{LiNbO}_3/\text{LiTaO}_3$ gives $\text{W}_{\text{Nb}}/\text{W}_{\text{Ta}}$ centers which are compensated for by lithium vacancies (V_{Li} ; niobium vacancies are expected to be energetically unfavorable due to the high negative charge). The decrease of the unit-cell volume has been related to the formation of cation vacancies.^{8,9} The ideal (LiNbO_3) structure will be stabilized by the defect centers, because the formation of anti-site defects (Nb_{Li}) is suppressed.¹

For low values of x , the energy levels of the greater part of the niobate/tantalate groups will hardly be influenced by the defect centers in the lattice, because their concentration is low. These samples show, in fact, a certain amount of intrinsic niobate/tantalate emission.

For higher x values, the influence of the defects on the luminescence properties increases: the intrinsic emission disappears, and emission bands with maxima at longer wavelengths become more important.

According to the literature,¹⁰ the extrinsic emission of LiNbO_3 peaks at about 520 nm ($\lambda_{\text{exc}} = 275 \text{ nm}$). The emission with a maximum at $\sim 530 \text{ nm}$, observed for $\text{Li}_{1-x}\text{Nb}_{1-x}\text{W}_x\text{O}_3$, is therefore ascribed to niobate groups next to lithium vacancies.

The $\text{Li}_{1-x}\text{Nb}_{1-x}\text{W}_x\text{O}_3$ solid solutions show a third emission band which is at even longer wavelengths than the extrinsic niobate emission. Its maximum depends strongly on x . Since there are no other types of (defect) niobate groups present, this emission is ascribed to the tungstate groups with an effective positive charge relative to the lattice.

Let us now compare these results with those for the isolated WO_6 octahedron. The emission and excitation bands of electronically isolated tungstate groups is at shorter wavelengths than observed here. For ordered tungstate perovskites A_2BWO_6 , for instance, the emission band peaks at about 450 nm ($\lambda_{\text{exc}} = \sim 275 \text{ nm}$) and is quenched at $\sim 200 \text{ K}$.¹⁸

However, tungstate excitation and emission bands shift to lower energies if oxygen corner-sharing between the WO_6 groups occurs. Proof for this comes from a study by Bode and Van Oosterhout.¹⁸ For ordered tungstate perovskites, next to intrinsic tungstate emission, another emission band at longer wavelengths was observed, which could be explained only by taking into account a small amount ($\sim 2\%$) of disorder between the cations. As a result the excitation and emission bands of these extrinsic WO_6 groups with other WO_6 groups as nearest neighbours shift to lower energies (longer wavelengths). The emission maximum lies at about 550 nm ($\lambda_{\text{exc}} = \sim 320 \text{ nm}$), and is quenched at room temperature.

In the oxide WO_3 all WO_6 octahedra are corner sharing. At 4.2 K the emission maximum lies at 680 nm ($\lambda_{\text{exc}} = 405 \text{ nm}$).¹⁹ The $T_{1/2}$ value of the luminescence is 65 K.¹⁹ The excited state of WO_3 is delocalized over the corner-sharing WO_6 octahedra, giving self-trapped exciton recombination.

So the spectral shift of the tungstate emission and excitation bands as a function of x in the system $\text{Li}_{1-x}\text{Nb}_{1-x}\text{W}_x\text{O}_3$ must be related to an increase in the amount of corner-sharing WO_6 groups.

Now the $\text{Li}_{1-x}\text{Ta}_{1-x}\text{W}_x\text{O}_3$ system is considered. Next to intrinsic tantalate emission, the $\text{Li}_{1-x}\text{Ta}_{1-x}\text{W}_x\text{O}_3$ solid

(15) Miller, R. C.; Nordland, W. A.; Bridenbaugh, P. M. *J. Appl. Phys.* 1971, 42, 4145.

(16) Weber, M. J., Ed. *CRC Handbook of Laser Science and Technology*; CRC Press: Boca Raton, FL, 1988; Vol. 3.

(17) Miller, R. C.; Savage, A. *Appl. Phys. Lett.* 1966, 9, 169.

(18) Bode, J. H. G.; Van Oosterhout, A. B. *J. Lumin.* 1975, 10, 237.

(19) Wiegell, M., unpublished results.

solutions also show an emission band at longer wavelengths. The maximum of this emission band depends on the excitation wavelength: for 290-nm excitation it lies at 540 nm, and for 320-nm excitation it lies at 580 nm (see also Figure 3).

Nonstoichiometric LiTaO_3 samples show extrinsic tantalate emission with a maximum at about 500 nm.¹² Not only the tantalate groups, but also the tungstate groups are expected to show luminescence at low temperatures. By varying the excitation wavelength the long-wavelength emission bands can be partly separated, but the spectral overlap is still large in contrast to what was observed for the $\text{Li}_{1-x}\text{Nb}_{1-x}\text{W}_x\text{O}_3$ system. By analogy with the niobate system the emission band with a maximum at 540 nm is ascribed to tantalate groups next to $\text{V}_{\text{Li}'}$, whereas the emission band with a maximum at 580 nm is ascribed to tungstate groups.

Since the emission band of the intrinsic TaO_6 group overlaps with the tungstate excitation band (see Figure 3), efficient energy transfer from the tantalate center to the tungstate center is to be expected. However, if we excite in the maximum of the tantalate excitation band (235 nm), only weak tungstate emission is found. This may be explained as follows: The 235-nm radiation is strongly absorbed, so that the surface layer is preferentially excited. If the surface concentration of W_{Ta} is low, the intensity of the tungstate emission will also be low. The 290-nm radiation penetrates deeper into the sample, because it is less absorbed at the surface. A strong tungstate emission is observed. Obviously the bulk concentration of the tungstate centers is much higher than their surface concentration. In the case of $\text{Li}_{1-x}\text{Nb}_{1-x}\text{W}_x\text{O}_3$ no energy transfer is to be expected, since the spectral overlap involved is small (see Figure 2).

In summary, the luminescence properties of $\text{Li}_{1-x}\text{Nb}_{1-x}\text{W}_x\text{O}_3$ and $\text{Li}_{1-x}\text{Ta}_{1-x}\text{W}_x\text{O}_3$ samples depend on x . This is in agreement with other studies,¹⁰⁻¹² which show that the luminescence of LiNbO_3 and LiTaO_3 depends strongly on the defect concentration.

Nonlinear Optical Properties. The total NLO response of the solid solutions $\text{Li}_{1-x}(\text{Nb}, \text{Ta})_{1-x}\text{W}_x\text{O}_3$ increases linearly with x (see Figures 4 and 5). Although the absorption edge shifts to longer wavelengths as x increases (see Figure 1), the NLO response is not influenced, since the fundamental absorption bands of the $\text{Li}_{1-x}(\text{Nb}, \text{Ta})_{1-x}\text{W}_x\text{O}_3$ samples still lie at much shorter wavelengths than the frequency doubled laser radiation (532 nm).

According to the bond parameter model derived by Bergman and Crane,⁶ the NLO response is a summation

of two contributions, i.e., one due to the Nb–O/Ta–O bonds and another due to the W–O bonds, since only the more covalent bonds contribute. We have, therefore, decomposed the total NLO response into a contribution due to the host lattice bonds and one due to the W–O bonds. The response due to the Nb–O/Ta–O bonds decreases linearly with x , whereas that due to the W–O bonds increases linearly with x (see Figures 4 and 5). Hence, the total SHG response shows a linear increase with x , since the Nb–O/Ta–O bonds are replaced by more polarizable W–O bonds. Moreover, we may also derive from these data that structural changes are of minor importance.

Using the bond parameter model,⁶ a value for β^{\parallel} of the W–O bonds of $(570 \pm 130) 10^{-40} \text{ m}^4/\text{V}$ was derived from the slopes of the “W–O” curves of Figures 4 and 5, neglecting β^{\perp} .

Bergman and Crane⁶ have also calculated β^{\parallel} values of several transition-metal oxo (TM–O) bonds, viz., $\beta^{\parallel}(\text{Ti–O}) = 337 \times 10^{-40}$, $\beta^{\parallel}(\text{Nb–O}) = (130 \pm 11) \times 10^{-40}$ and $\beta^{\parallel}(\text{Ta–O}) = (81 \pm 2) 10^{-40} \text{ m}^4/\text{V}$ (with $d_{36}(\text{KH}_2\text{PO}_4) = 0.63 \text{ pm}/\text{V}$).¹⁶ When comparing these β^{\parallel} values to $\beta^{\parallel}(\text{W–O})$, the following relations are found: $\beta^{\parallel}(\text{W–O}) \cong 1.7 \times \beta^{\parallel}(\text{Ti–O})$, $\beta^{\parallel}(\text{W–O}) \cong 4 \times \beta^{\parallel}(\text{Nb–O})$, and $\beta^{\parallel}(\text{W–O}) \cong 7 \times \beta^{\parallel}(\text{Ta–O})$. Thus the value of $\beta^{\parallel}(\text{W–O})$ is quite large with respect to the other TM–O bond polarizabilities.

However, this can be explained as follows: Recently Lines,²⁰ based on the work of Harrison,²¹ has derived an expression for the nonlinear optical bond polarizability β^{\parallel} of transition-metal oxo compounds. It appears that β^{\parallel} , among others, is inversely proportional to the square of the mean bandgap (denoted as E_g).²⁰

Figure 1 shows that the optical absorption edge, which is a measure of the optical bandgap, of the $\text{Li}_{1-x}(\text{Nb}, \text{Ta})_{1-x}\text{W}_x\text{O}_3$ samples strongly depends on x : it shifts to longer wavelengths as x increases. Thus the optical bandgap of the samples decreases as x increases. For instance, for $\text{Li}_{1-x}\text{Nb}_{1-x}\text{W}_x\text{O}_3$ the optical bandgap changes from 5.0 eV ($x = 0$) to 3.4 eV ($x = 0.5$). So in view of this large difference in bandgap, $\beta^{\parallel}(\text{W–O})$ is expected to be at least a factor 2 larger than $\beta^{\parallel}(\text{Nb–O})$.

In conclusion, the increase of the SHG response of the $\text{Li}_{1-x}(\text{Nb}, \text{Ta})_{1-x}\text{W}_x\text{O}_3$ solid solutions with x is ascribed to the introduction of the more covalent W–O bonds.

Acknowledgment. This work was supported by Philips Research Laboratories, Eindhoven.

(20) Lines, M. E. *Phys. Rev. B* 1991, 43, 11978.

(21) Harrison, W. A. *Electronic Structure and the Properties of Solids*; Freeman: San Francisco, 1980.